A Novel Fluorescence-activated Cell Sorter–Based Screen for Yeast Endocytosis Mutants Identifies a Yeast Homologue of Mammalian eps15

Beverly Wendland, J. Michael McCaffery, Qin Xiao, and Scott D. Emr

Division of Cellular and Molecular Medicine and Howard Hughes Medical Institute, University of California at San Diego, School of Medicine, La Jolla, California 92093-0668

Abstract. A complete understanding of the molecular mechanisms of endocytosis requires the discovery and characterization of the protein machinery that mediates this aspect of membrane trafficking. A novel genetic screen was used to identify yeast mutants defective in internalization of bulk lipid. The fluorescent lipophilic styryl dye FM4-64 was used in conjunction with FACS® to enrich for yeast mutants that exhibit internalization defects. Detailed characterization of two of these mutants, *dim1-1* and *dim2-1*, revealed defects in the endocytic pathway. Like other yeast endocytosis mutants, the temperature-sensitive *dim* mutants were unable to endocytose FM4-64 or radiolabeled α-factor as efficiently as wild-type cells. In addition, double mutants with either *dim1-Δ* or *dim2-1* and the endocytosis mutants *end4-1* or *act1-1* displayed synthetic growth defects, indicating that the *DIM* gene products function in a common or parallel endocytic pathway. Complementation cloning of the *DIM* genes revealed identity of *DIM1* to *SHE4* and *DIM2* to *PAN1*. Pan1p shares homology with the mammalian clathrin adaptor–associated protein, eps15. Both proteins contain multiple EH (eps15 homology) domains, a motif proposed to mediate protein–protein interactions. Phalloidin labeling of filamentous actin revealed profound defects in the actin cytoskeleton in both *dim* mutants. EM analysis revealed that the *dim* mutants accumulate vesicles and tubulo-vesicular structures reminiscent of mammalian early endosomes. In addition, the accumulation of novel plasma membrane invaginations where endocytosis is likely to occur were visualized in the mutants by electron microscopy using cationized ferritin as a marker for the endocytic pathway. This new screening strategy demonstrates a role for She4p and Pan1p in endocytosis, and provides a new general method for the identification of additional endocytosis mutants.

THE plasma membrane of cells acts as an interface between the cell and the extracellular environment, and serves as an important site for communication and transduction of environmental stimuli into appropriate cellular responses. The regulation of exocytosis and endocytosis is crucial for maintaining the appropriate composition, function, and surface area of the plasma membrane during the continuous trafficking of lipids and proteins to and from this essential cellular domain.

In mammalian cells, endocytosis is responsible for both internalization of nutrients such as iron (Hemmaplardh and Morgan, 1976; Karin and Mintz, 1981) and cholesterol (Anderson et al., 1977), as well as downregulation of activated receptor–ligand complexes. There are believed to be at least three forms of endocytosis: clathrin dependent, clathrin independent, and phagocytosis (Lamaze and Schmid, 1995). The best characterized mechanism is clathrin-dependent endocytosis, in which receptors are first concentrated into clathrin-coated pits via an interaction between the cytoplasmic tail of the receptor and clathrin adaptor proteins, followed by the association of clathrin triskelions with the adaptor proteins (reviewed in Pearse and Crowther, 1987). The clathrin triskelions can self-assemble in vitro, and this property is thought to provide the mechanical force that bends the plasma membrane into a budding coated vesicle. After budding is completed, the coat is disassembled, and the adaptors and clathrin triskelions are recycled back through the cytoplasm to reassemble at a new coated pit. The uncoated vesicle then fuses with an endosome before the contents are ultimately delivered to the lysosome, and the vesicular membrane is degraded or recycled to other membrane destinations. Clathrin-independent endocytosis is less well understood, but may be mediated by two classes of vesicles: "noncoated" vesicles and caveolae (also known as plasmalemmal vesicles; Palade, 1953; Rothberg et al., 1992). Finally, phagocytosis is a more specialized form of endocytosis that involves the bulk internalization of particles by an actin-dependent engulfment process (West et al., 1989; Hewlett et al., 1994). In addition to the well-characterized function of clathrin in endocytosis, a general role for actin in the internalization

Address all correspondence to Scott D. Emr, Division of Cellular and Molecular Medicine, Howard Hughes Medical Institute, University of California at San Diego, School of Medicine, La Jolla, CA 92093-0668. Tel.: (619) 534-6462. Fax: (619) 534-6414.

of caveolae (Parton et al., 1994) and in apical endocytosis in MDCK cells (Gottlieb et al., 1993) has also been demonstrated. There are many questions that remain, however, in clarifying the details of both clathrin-dependent and -independent modes of internalization.

As an approach to elucidate important molecules and events required for endocytosis, genetic screens using the budding yeast *Saccharomyces cerevisiae* have been used. Consistent with observations in mammalian cells, many of the gene products identified in these screens reveal a requirement for proteins of the actin cytoskeleton; these proteins include actin (Kubler and Riezman, 1993; Munn et al., 1995), the putative cytoskeletal proteins End3p and End4p (Raths et al., 1993; Benedetti et al., 1994), and the fimbrin homologue Sac6p (Kubler and Riezman, 1993). In addition, important roles for the amphiphysin homologues Rvs161p/End6p and Rvs167p (Munn et al., 1995), calmodulin (Kubler et al., 1994), and type I myosins (Geli and Riezman, 1996) in the internalization step of the yeast mating pheromone α-factor have been reported. Screens for *end* mutants generally have assayed for defects in the internalization of mating pheromone–receptor complexes, a process that at least partially depends on the function of clathrin heavy chains (Tan et al., 1993). However, yeast cells deleted for the gene encoding clathrin heavy chain are viable, (Payne and Schekman, 1985), but these strains internalize mating pheromone receptors at a much reduced rate relative to wild-type cells (Payne et al., 1988). This suggests that, as in mammalian cells, clathrin-independent modes of endocytosis exist in yeast.

Flow cytometry was used previously to describe the endocytosis kinetics of fluorescently labeled histone in CHO cells (Murphy et al., 1982), and more recently, in a screen for endocytosis mutants in mammalian cells using fluorescently labeled transferrin as a marker for recycling endosomes (Cain et al., 1991). These studies demonstrate the use of a FACS®-based approach for a detailed analysis of endocytosis in a population of cells, as well as for the isolation of mutants in the endocytic pathway. We report a novel screen for endocytosis mutants in yeast, using the lipophilic styryl dye *N*-(3-triethylammoniumpropyl)-4-(p-diethylaminophenylhexatrienyl) pyridium dibromide (FM4-64)[1] to follow bulk internalization of plasma membrane (Vida and Emr, 1995). Unlike previous selections, this screen was designed to isolate mutants defective in membrane uptake, a common feature of all pathways of endocytosis. FM4-64 is a suitable probe for this screen because it is an endocytic tracer that travels from the plasma membrane to the vacuolar membrane via punctate cytoplasmic intermediates in a time-, temperature-, and energy-dependent manner (Vida and Emr, 1995). We report the isolation of many new candidate endocytosis mutants, as well as the detailed characterization of two of these mutants, *dim1-1* and *dim2-1*. Both characterized *dim* mutants exhibit reduced internalization of FM4-64 and the mating pheromone α-factor; additionally, actin localization is disrupted in both *dim* mutants. Cloning and sequencing revealed identity of *DIM1* with *SHE4* and of *DIM2* with *PAN1*. So far, no function has been described for *PAN1*, but the sequence contains motifs that are present in the mammalian clathrin adaptor–associated protein eps15, as well as in yeast End3p, another protein that is required for endocytosis (Raths et al., 1993; Benedetti et al., 1994). The *dim* mutants were found to accumulate aberrant membranous structures, including vesicles and tubules that might represent exaggerated intermediates in an endocytic pathway. Preliminary studies examining the internalization of cationized ferritin highlight a route of endocytosis via plasma membrane invaginations that is highly exaggerated in the *dim* mutants.

1. *Abbreviations used in this paper*: EH, eps15 homology; EMS, ethyl methanesulfonate; FM-64, *N*-(3-triethylammoniumpropyl)-4-(p-diethylaminophenylhexatrienyl) pyridinium dibromide; v-ATPase, vacuolar ATPase.

Materials and Methods

Strains and Media

Bacterial strains were grown on standard media (Miller, 1972). The genotypes of *Escherichia coli* strains used were XL1Blue [*supE44 thi-1 lac endA1 gyrA96 hsdR17 relA1 F'proAB lacI^q ZΔM15*] (Bullock et al., 1987) and JM101 [*Δ(lac-pro) supE thi-1 F'traD36 lacI^q ZΔM15 proAB*] (Yanisch-Perron et al., 1985).

Saccharomyces cerevisiae yeast strains used (Table I) were grown in standard YPD, SD minimal, and sporulation media (Sherman et al., 1979).

Materials

N-(3-triethylammoniumpropyl)-4-(p-diethylaminophenylhexatrienyl) pyridinium dibromide (FM4-64) and rhodamine phalloidin were purchased from Molecular Probes, Inc. (Eugene, OR). $^{35}SO_4$, and Trans^{35}S label were obtained from ICN Radiochemicals (Irvine, CA). Restriction enzymes, T4 DNA ligase and polymerase, Klenow enzyme, and alkaline phosphatase were acquired from Boehringer Mannheim Biochemicals (Indianapolis, IN) or New England Biolabs (Beverly, MA). Sequenase sequencing kits 5-bromo-4-chloro-3-indoyl-β-D-galactoside and isopropyl-β-D-thiogalactoside were from U.S. Biochemical Corp. (Cleveland, OH), and [α-^{35}S]dATP was acquired from Amersham Corp. (Arlington Heights, IL). Glusulase was from DuPont (Wilmington, DE), and Zymolyase-100T was purchased from Seikagaku Kogyo (Tokyo, Japan). Sephacryl S-1000 was from Pharmacia (Uppsala, Sweden). All other chemicals were obtained from Sigma Chemical Co. (St. Louis, MO).

Mutagenesis, FM4-64 Labeling, and FACS® Analysis

Ethyl methanesulfonate (EMS) mutagenesis of wild-type SEY6210 was performed as described (Rose et al., 1990), and 22–25% viability was obtained using this procedure. The mutagenized cells were diluted in YPD and grown overnight at 22°C. A 1-h preincubation at 38°C was followed by a 10-min labeling with 16 μM FM4-64 (1:100 dilution of stock; 1.6 μM FM4-64 in DMSO) and a 1-h chase. The cells were then subjected to a sterile sort on a FACStar® fluorescence-activated cell sorter (Becton Dickinson & Co., Mountain View, CA), and cells of low fluorescent intensity were collected and plated on YPD at 26°C. Replica plating to 38°C permitted analysis of the percent of surviving colonies that were temperature sensitive for growth. Individual colonies were labeled with FM4-64 and chased at 38°C, allowing identification of *dim* mutants. After several back-crosses to SEY6210 and SEY6211, strains BWY1, BWY2, BWY10, BWY11, and BWY16 were generated carrying *dim1-1* or *dim2-1* alleles. FM4-64 labeling of *dim* mutants was performed as described (Vida and Emr, 1995), except that cells were grown in YNB plus appropriate amino acids and were diluted 1:1 with YPD before the temperature shift to 38°C. FM4-64 was used at 16 and 32 μM for 38°C and 26°C labeling, respectively. Images were acquired under identical conditions using a CCD camera (model 4995; COHU, San Diego, CA), an integrator box (model 440A; Colorado Video Inc., Boulder, CO), and an LG-3 Frame Grabber (Scion Corp., Frederick, MD). The software used was NIH Image 1.55 and Adobe Photoshop 3.0.

Cloning of the DIM1 and DIM2 Genes

For cloning of the *DIM1* gene, a *LEU2-CEN S. cerevisiae* genomic library

(in the *E. coli* yeast shuttle vector YCp50, *CEN4 ARS1 URA3*; Rose et al., 1987) was transformed into BWY1, replica plated to 38°C, and colonies that were temperature resistant were selected for plasmid rescue. Eight colonies representing three different genomic inserts were isolated from BWY1 temperature-resistant cells and retransformed into BWY1 to confirm plasmid linkage. Restriction mapping and subcloning narrowed the complementing region to a BglII-BamHI fragment (pDIM1, also known as pSHE4, BglII-BamHI fragment in pRS414 *TRP1 CEN*) that was sequenced on both strands using the Sequenase kit, revealing a 2,367-bp open reading frame predicting a 789–amino acid protein. 321 bp of the 5′ end of the neighboring *PEP12* gene was also included in this fragment. A deletion construct was generated by cloning the BglII/BamHI fragment into the BamHI site of pBluescript KSII(−) (Stratagene, La Jolla, CA) and inserting the *HIS3* gene into the ClaI and BstBI sites, which removes 92% of the open reading frame (pDIM1Δ2). This construct was linearized with PvuII and BstYI (which cuts at the site generated by the BglII-BamHI ligation), and was transformed into the wild-type strains SEY6210, SEY6211, and SEY6210.5, generating BWY6, BWY7, and BWY5, respectively. PCR analysis using oligonucleotides outside the linearization sites confirmed the deletion of the *DIM1* gene. An additional deletion replacing the Eco47III-NsiI fragment with *LEU2* (pDIM1Δ1) removed 17% of the open reading frame and also resulted in a null phenotype. The integrative mapping construct was generated by cloning the BglII-BamHI fragment into pRS304 (pDIM1-MAP), which contains the *TRP1* gene and no sequences for maintenance of plasmid replication in yeast. This construct was linearized with NsiI, transformed into BWY3 (generating BWY4), sporulated, and dissected.

To clone the *DIM2* gene, a *LEU2-CEN S. cerevisiae* genomic library was transformed into BWY10, replica plated to 38°C, and colonies that were temperature resistant were selected for plasmid rescue. Three colonies representing two different genomic inserts were isolated from temperature-resistant BWY10 colonies and retransformed into BWY10 cells to confirm plasmid linkage. Restriction mapping and subcloning narrowed the complementing region to an XmnI-DraI fragment (pDIM2, also known as pPAN1, the XmnI-DraI fragment in pRS415 *LEU2 CEN*). Both ends of two EcoRI fragments were sequenced that revealed identity of the *DIM2* gene with *PAN1*. Using oligonucleotides and subcloning for further sequencing across regions of incongruity between *PAN1* and YIR006c (the same genomic region identified by the yeast genome project) showed identity with YIR006c. For the *PAN1* disruption construct (pPAN1-KO), the 4.4-kb SalI-BamHI fragment was subcloned into pBluescript cut with SalI and BamHI, followed by insertion of the *HIS3* gene into the EcoRV sites of *PAN1* and linearization with SalI and BamHI for integration into SEY6210.5, generating BWY14. Integrative mapping was done using the BglII fragment subcloned into pRS303 cut with BamHI to generate pPAN1-MAP, which was linearized using NcoI and transformed into BWY12 to produce BWY13.

α-Factor Internalization and Degradation

Radiolabeled α-factor was produced according to the method of Dulic et al. (1991) and used in internalization and degradation assays performed essentially as described, with the following exceptions: unbound α-factor was removed with one wash of binding buffer at 4°C, followed by a preincubation at 26°C or 38°C for 20–30 min. To initiate internalization, the cells were diluted to 30 OD/ml by the addition of 4 vol of prewarmed 1.25× YPD and 5% glucose. Experiments were performed two to three times with each strain. Strains BWY17, BWY15, and BWY9 were used. BWY15 was generated by crossing BWY10 with a wild-type strain harboring a *bar1-1* allele.

Generation of Double Mutants for Genetic Interaction Studies

For *vma4-Δ dim* double mutants, KMY1004α was mated with BWY1 and BWY10, sporulated, and dissected onto YPD-MES, pH 5.5, plates for germination. For other double mutants, spores were germinated on YPD plates at 26°C, except for *end4* doubles, which were germinated at room temperature. DBY1691 was mated with BWY6 and DBY1692 with BWY10 to generate *act1-1 dim* double mutants. RH268-1C was crossed to BWY6 and BWY10 to produce *end4-1 dim* double mutants. *DIM1* deletions were introduced into YAS1114, YAS1115, GPY1000α, and GPY418 by integrating pDIM1Δ1(*LEU2*). 10–20 tetrads were dissected in each case, and the identification of alleles contained within a germinated spore was confirmed by back-crossing with parental strains and testing resultant diploids for homozygosity.

Phalloidin Labeling of Filamentous Actin and Bud Scar Staining

Mid–log phase cells SEY6210.5, BWY8, BWY12, SEY6210, BWY6, BWY10, YAS1114, and YAS1115 were grown at 26°C, a portion shifted to 38°C for 2.5 h, and then fixed and stained with Calcofluor White M2R (Sigma) or phalloidin as described (Benedetti et al., 1994).

Purification of Clathrin-coated Vesicles

Vesicles were isolated from SEY6210 and BWY6 as described (Mueller and Branton, 1984). 1 ml of every fifth fraction was precipitated with 10% TCA with the addition of insulin as carrier. The proteins were resolved by SDS-PAGE, immunoblotted, and Chc1p was detected using the mAb SKL1 (Lemmon et al., 1988) at a 1:2,000 dilution. The data represent at least two independent experiments for each strain. The indicated fractions were fixed with 3% glutaraldehyde, pelleted at 100,000 *g* for 1 h, and processed for routine morphology EM as described below.

EM and Cationized Ferritin Internalization

Conventional EM for routine morphology was performed as described (Rieder et al., 1996) on SEY6210, BWY6, and BWY16 grown at 26°C, and on a portion shifted to 38°C for 90 min. The same strains, as well as RH268-1C, YAS1114, and YAS1115, were used for cationized ferritin internalization. 15-OD cells were converted to spheroplasts at 26°C in spheroplasting buffer (1.2 M sorbitol, 10 mM Tris, pH 7.5, 10 mM $CaCl_2$, 2 mM DTT, 0.6 mM PMSF, 0.1–1.0 mg/ml Zymolyase-100T), washed twice (1.2 M sorbitol, 100 mM MES, pH 6.5, 0.5 mM $MgCl_2$, 1 mM EGTA, 0.2 mM DTT, 0.6 mM PMSF), and resuspended in 1.11× internalization buffer (1.11× YNB, 2.22% glucose, 1.33 M sorbitol, 1.11× amino acids) at 8.3 OD/ml. A preincubation at the appropriate temperature for 30 min was followed by the addition of 0.2 ml 10 mg/ml cationized ferritin and continued incubation for 30 min. The cells were gently pelleted, resuspended in fixative (2% glutaraldehyde, 1.2 M sorbitol, 5mM $MgCl_2$, 5 mM $CaCl_2$, 97 mM cacodylate, pH 7.4), and processed as described above for EM with the exception of poststaining with uranyl acetate and lead citrate.

Results

FACS® Isolation of dim Mutants

The lipophilic dye FM4-64 has been shown to be a useful probe for endocytosis in yeast (Vida and Emr, 1995). We exploited these observations in an enrichment protocol to identify endocytic mutants: the endocytosis mutants *end3-1* and *end4-1* were found to internalize less fluorescent dye than wild-type cells (two- to fourfold reduction in fluorescent signal in the vacuolar membrane, data not shown), and therefore endocytosis mutants could be easily sorted by FACS®.

As an initial test of the feasibility of this approach, we tested whether cells that bind but do not endocytose the dye could be stripped of uninternalized, plasma membrane–localized FM4-64. Cells were incubated with FM4-64 at 0°C to allow insertion of the dye into the plasma membrane, followed by washing at 0°C. For comparison, cells were also incubated with FM4-64 at 30°C, followed by a wash and a 60-min chase period, during which FM4-64 is internalized and transported to the vacuole (Vida and Emr, 1995). The samples were then subjected to analysis by FACS®. The cells that were labeled and washed at 0°C (Fig. 1 *A*) revealed a low level of fluorescence that was nearly identical to that observed in unincubated cells (data not shown). The cells with internalized FM4-64 displayed ~10 times greater fluorescence intensity (Fig. 1 *B*), which

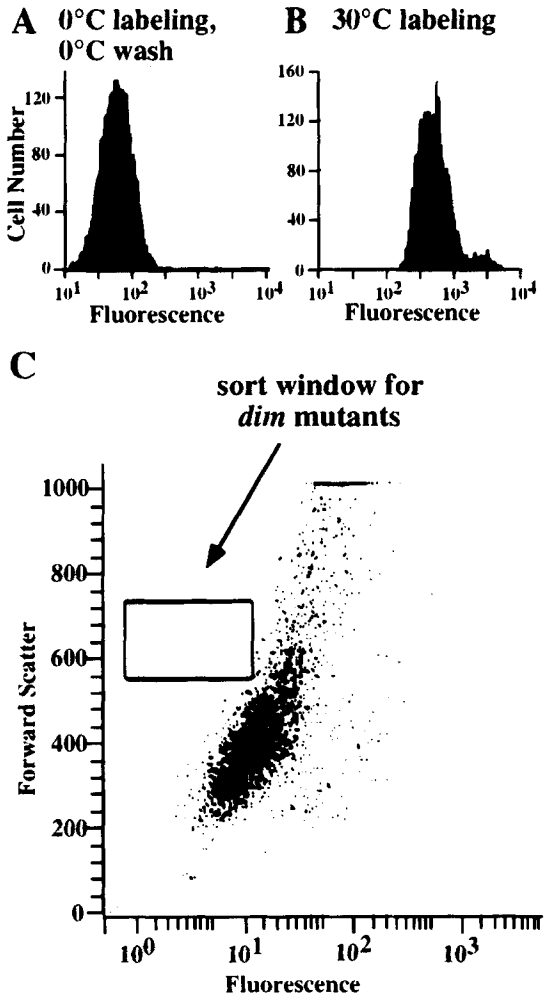

Figure 1. FACS® of FM4-64–labeled yeast. (*A*) Wild-type SEY6210 was labeled with FM4-64 on ice to restrict the dye to the plasma membrane, and was then washed four times with ice-cold medium to extract the dye, followed by FACS® analysis. (*B*) SEY6210 was labeled and chased at 30°C to allow internalization from the plasma membrane to the vacuole, followed by FACS® analysis. (*C*) SEY6210 cells were mutagenized with EMS, incubated at 38°C for 1 h, labeled with FM4-64 for 10 min, and chased for 1 h. A FACS® sort was performed, and cells falling into the "dim" window were collected for further analysis.

was equivalent to the signal observed in cells labeled at 0°C and not washed (data not shown). This demonstrated that plasma membrane–localized FM4-64 could be efficiently stripped from cells, and that FACS® analysis can be used to discriminate cells that endocytose FM4-64 versus those that do not.

To screen for endocytosis mutants, wild-type cells were mutagenized with EMS and were allowed to recover in rich medium at 22°C for 12 h. The level of EMS mutagenesis used resulted in an ~80% kill rate, and, of the survivors, 10% were temperature sensitive for growth. The mixed population of cells was then incubated at 38°C for 1 h, followed by a 10-min incubation with FM4-64 and a 1-h chase period at 38°C. Under these conditions, wild-type cells internalize FM4-64 to the vacuole (see below). The temperature shift was performed to allow for the isolation of temperature-conditional alleles of genes required for endocytosis and possibly also for growth, and does not exclude the isolation of genes that are not essential. The labeled and chased cells (1×10^7) were then subjected to FACS® and selected from a window of low fluorescent intensity (Fig. 1 *C*, sort window). Approximately 0.05% of the total cells (4,894) were selected by this window, of which 602 yielded viable colonies. 25% of cells selected by FACS® were temperature sensitive for growth, a greater than twofold enrichment relative to the unsorted population.

100 colonies were tested individually for the ability to internalize FM4-64 after a 1-h preshift to 38°C. 10 colonies displayed less intense labeling of the vacuole, referred to as the "dim" phenotype. Two of these mutants that also were temperature sensitive for growth were characterized further. In both, the "dim" phenotype and the temperature sensitivity cosegregated through three back-crosses to the parental strain. The two mutants contained mutations in distinct loci: a diploid strain generated by mating the two mutants resulted in wild-type levels of FM4-64 internalization, whereas homozygous mutant diploids were "dim" (data not shown).

dim1 and dim2 Cells Exhibit Endocytosis Defects

The fluorescent lipophilic styryl dye FM4-64 is useful as a marker to observe the function of the endocytic pathway in yeast. Reduced fluorescent intensity in the vacuolar membrane would presumably correspond to a reduction in endocytic flow from the plasma membrane to the vacuole. We therefore analyzed uptake of FM4-64 in the *dim* mutants at both 26°C and 38°C in cells that either did or did not harbor single-copy plasmids encoding wild-type copies of the *DIM* genes (see below). Identical exposure parameters were used when acquiring images to allow fluorescent intensity comparisons. When the labeling was performed at 26°C, vacuolar labeling in *dim1-Δ* and *dim2-1* cells was slightly less than wild-type levels (Fig. 2, 26°C). Labeling that was performed after a 30-min preincubation at 38°C followed by 45 min of chase revealed diminished vacuolar staining and the appearance of punctate structures (Fig. 2, 38°C, 30 min). When a 1-h preshift to 38°C preceded the labeling, the majority of the signal was restricted within punctate structures (Fig. 2, 38°C, 60 min). Even after 2.5 h of chase, the signal was still observed in the punctate structures and did not chase to the vacuolar membrane (data not shown). A temperature-dependent phenotype for a deletion strain was not expected, but has been reported for other deletions (e.g., temperature-sensitive polarized secretion in *tpm1-Δ*; Liu and Bretscher, 1992). In addition, when the *dim* mutants are incubated at elevated temperatures, only a single large vacuole is seen rather than the three to five smaller vacuoles that are observed in wild-type and complemented mutant cells (Fig. 2). However, processing and sorting of the soluble vacuolar hydrolase carboxypeptidase Y is normal in both *dim* mutants (data not shown), indicating that their ER to vacuole transport pathway is unaffected. As anticipated, based on the selection scheme used for their isolation, *dim1-Δ* and *dim2-1* cells exhibited approximately two- to fourfold reduced fluorescent intensity of FM4-64 at 38°C when compared to

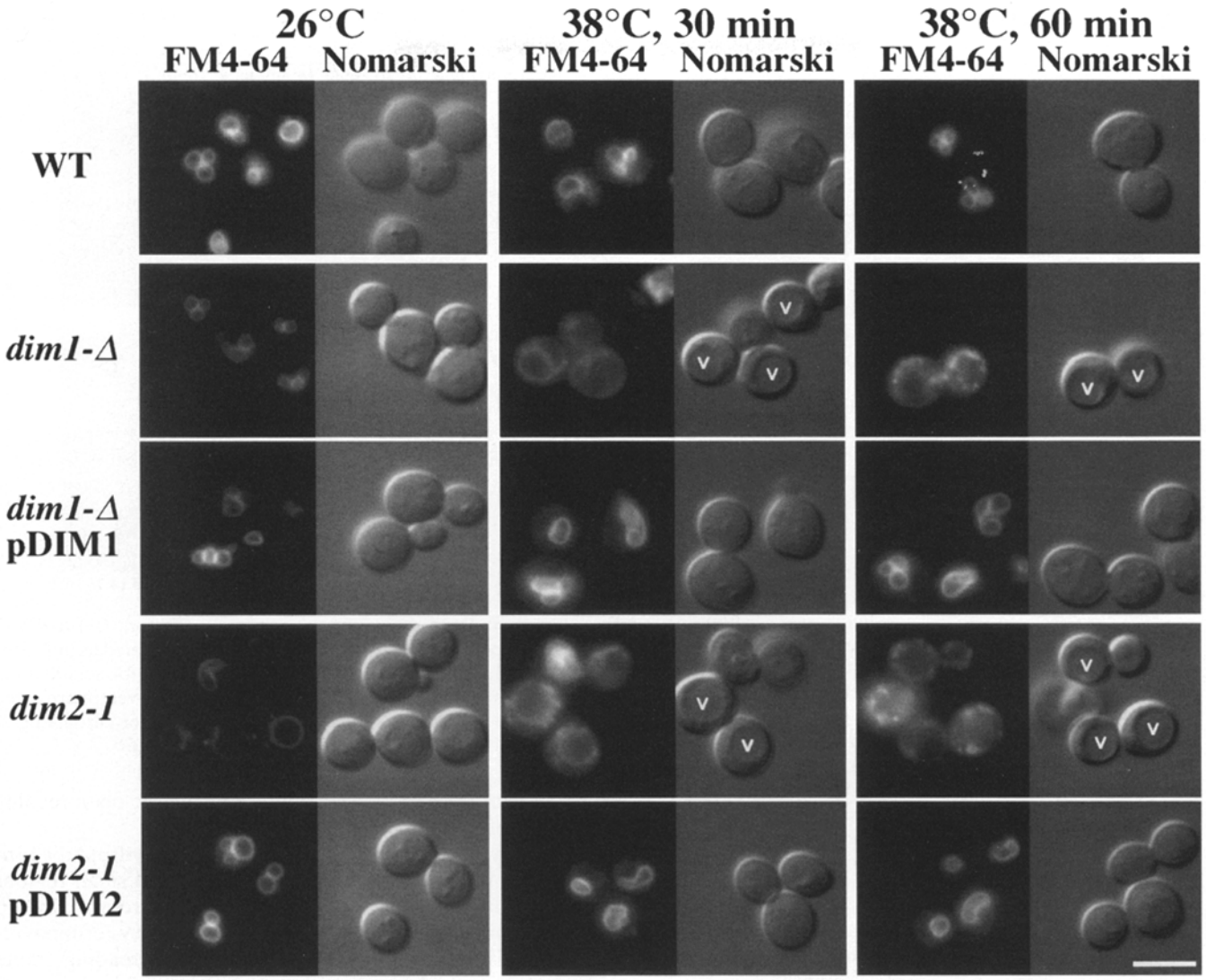

Figure 2. FM4-64 labeling of wild-type and *dim* mutants. SEY6210 (wild-type), BWY6 (*dim1-Δ*) with or without complementing pDIM1 plasmid, and BWY10 (*dim2-1*) with or without complementing pDIM2 plasmid cells were labeled at 26°C for 20 min, followed by a 90-min chase, and were preincubated at 38°C for 30 min, labeled for 10 min, and chased for 45 min; or were preincubated at 38°C for 1 h, labeled for 10 min, and chased for 45 min. Images were acquired under identical conditions to compare fluorescent intensities. Vacuoles (*V*) are indicated in Nomarski panels of the uncomplemented *dim* mutants. Bar, 5 μm.

the intensity of wild type cells, and this internalization defect was rescued by the presence of the *DIM1* or *DIM2* cloned genes, respectively.

The *dim* phenotype is consistent with defects in the trafficking of bulk lipid. As an alternative assay for endocytic defects in *dim1-Δ* and *dim2-1* mutants, internalization of the yeast-mating pheromone α-factor serves as a simple measure of receptor-mediated endocytosis (Dulic et al., 1991). In this experiment, α-factor was bound to the surface of the cells, and internalization was initiated at time 0 by the addition of glucose. At 38°C, *dim1-Δ* cells had a two to threefold reduction in the kinetics of α-factor internalization relative to that observed in *dim1-Δ* cells at 26°C or in wild-type cells (Fig. 3, *A* and *B*). The initial rate of internalization appeared to be even slower in the *dim2-1* mutant at 38°C (Fig. 3 *C*). These defects were rescued to nearly wild type kinetic rates when *dim1-Δ* or *dim2-1* cells harboring complementing plasmid were assayed (data not shown).

Further analysis of α-factor internalization in *dim1-Δ* cells involved examining the fate of internalized α-factor. In wild type cells, internalized α-factor is delivered to the vacuole, where it is degraded by vacuolar proteases (Singer and Riezman, 1990). Consequently, the arrival of α-factor in the vacuole is monitored by assessing its degradation. Internalization of radiolabeled α-factor experiments were performed, followed by processing for TLC to visualize α-factor degradation. In *dim1-Δ* cells, at a permissive temperature, cell-associated α-factor was cleared/internalized nearly as rapidly as in wild-type cells (Fig. 4, *A* and *B*, lanes *1–8*). When the cells were incubated at 38°C for 30 min before internalization, however, the α-factor in *dim1-Δ* cells was stabilized in the intact form (Fig. 4, *A* and *B*, lanes *11* and *12*) and very little α-factor was observed in

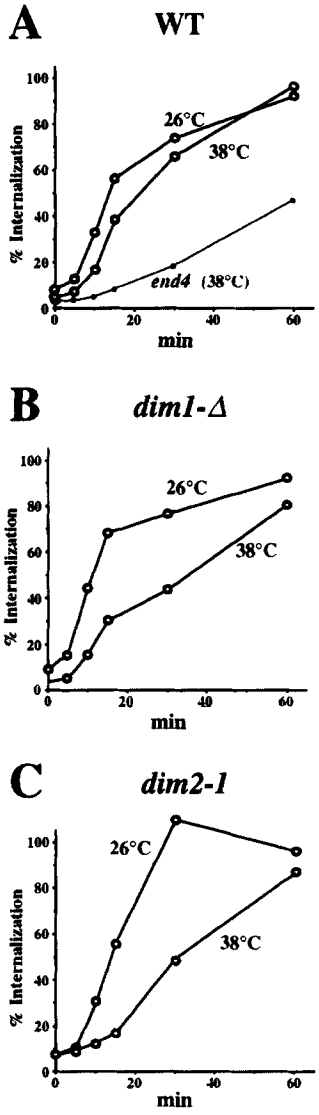

Figure 3. α-factor internalization in wild-type and *dim* mutants. (*A*) BWY17 (wild-type), (*B*) BWY9 (*dim1-Δ*), and (*C*) BWY15 (*dim2-1*) cells were incubated with radiolabeled α-factor at 0°C to allow binding to surface receptors, washed of unbound label, preincubated at 26°C or 38°C for 30 min, and glucose was added at time 0 to initiate internalization. At the indicated time points, aliquots were withdrawn and diluted in ice-cold buffer at pH 6.2 (total α-factor, surface-bound plus internalized) or pH 1.1 (internalized α-factor, acid wash to dissociate surface-bound α-factor). The samples were then filtered, counted by scintillation, and the results were plotted as the ratio of pH 1/pH6 counts for each time point to represent the percent of internalized α-factor. The data represent the average of two experiments.

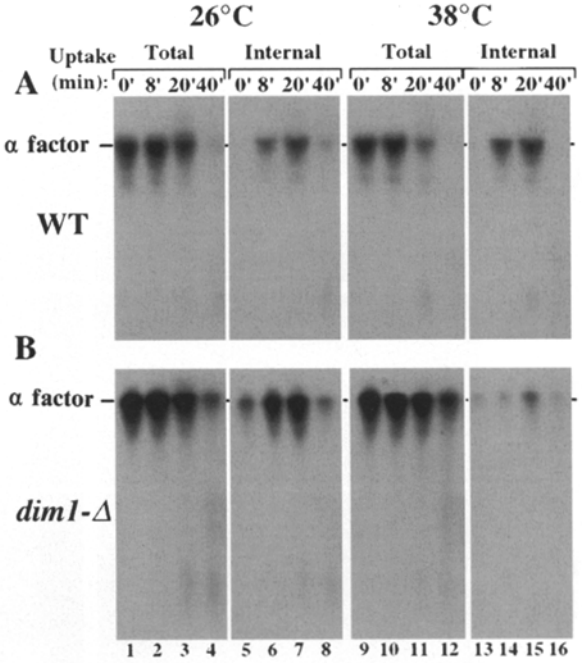

Figure 4. Degradation of internalized α-factor. (*A*) BWY17 (wild-type) or (*B*) BWY9 (*dim1-Δ*) cells were treated as indicated in Fig. 3, but rather than filtering the samples for scintillation, they were pelleted, washed, and lysed to recover internalized α-factor. The samples were resolved by thin-layer chromatography to differentiate mature from degraded α-factor.

the internal fraction of these cells (Fig. 4 *B*, lanes *13–16*). Together, these experiments indicate that *dim* mutants exhibit a significant reduction in the endocytosis of both bulk lipids and α-factor, and that these defects are exaggerated at a high temperature.

Cloning and Characterization of the DIM1 and DIM2 Genes: Identity with SHE4 and PAN1

The *DIM1* gene was cloned by complementation of the temperature sensitive for growth phenotype of the *dim1-1* mutant. To do this, *dim1-1* cells were first transformed with a genomic *CEN-LEU2* library (Rose et al., 1987) and plated at 26°C. Colonies were then replica plated and grown at 26°C or 38°C. Colonies that could survive at 38°C were chosen, and plasmid DNA was rescued from them. Three distinct but overlapping library plasmids that were capable of rescuing the growth defect were subjected to restriction mapping, and a region of overlap was determined. A minimum complementing BglII/BamHI fragment (Fig. 5 *A*) rescued both the growth and the FM4-64 internalization defects of *dim1-1* cells. Both strands of this fragment were sequenced, and a single large open reading frame of 789 amino acids was detected.

Analysis of the *DIM1* gene predicted a hydrophilic protein sequence. Database searches indicated small regions of similarity to the yeast dynamin–like protein Dnm1p (Gammie et al., 1995) and also to the carboxy-terminal region of the *Caenorhabditis elegans* open reading frame yk44f2.5, which predicts a 961–amino acid protein with 38% identity to heat shock protein–binding immunophilins (Callebaut et al., 1992) in the amino-terminal 43–115 residues. During the course of this work, *SHE4*, isolated as a gene necessary for Swi5p-dependent HO expression, was reported in the database (Jansen et al., 1996), as was the chromosome XV open reading frame OR26.26 (*Saccharomyces* Genome Database). Both are identical to *DIM1*, with the exception that *SHE4* is predicted to encode a 791–amino acid protein. This difference is likely caused either by strain variations or sequencing errors. Hereafter, *DIM1* will be referred to as *SHE4* and the *dim1-1* allele as *she4-1*.

Integrative mapping confirmed that the *SHE4* gene corresponded to the *she4-1* locus. To determine if *SHE4* was essential, a disruption construct in which 92% of the *SHE4* gene was replaced by the *HIS3* gene was generated (Fig. 5 *A*). The construct was used to disrupt one genomic copy of *SHE4* in a wild-type diploid strain. The resulting strain was then sporulated, and 20 tetrads were dissected. Germination of the meiotic products at 30°C yielded four viable haploid colonies (data not shown), indicating that *SHE4* is not an essential gene. We also constructed haploid *she4-Δ* null strains that, like *she4-1*, are temperature sensitive for growth (Fig. 5 *B*) and display the *dim* pheno-

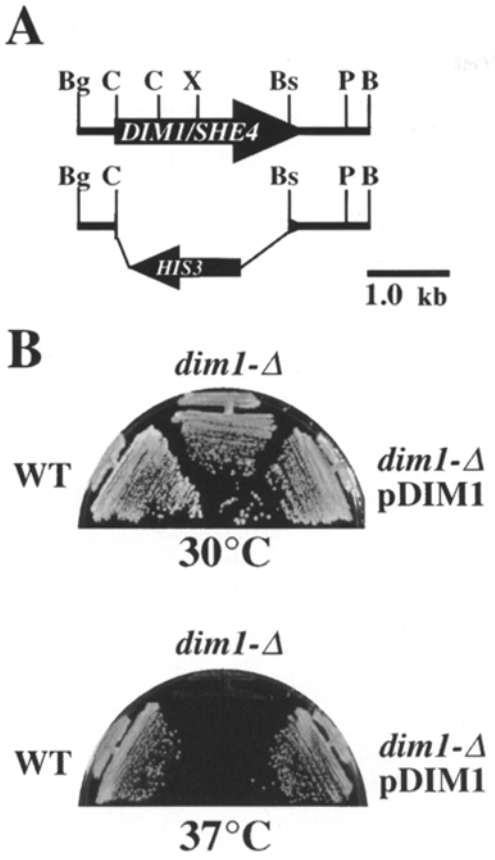

Figure 5. Analysis of the *SHE4/DIM1* gene. (*A*) A 10-kb genomic fragment that complemented the growth defect of BWY1 (*dim1-1*) cells was isolated. The 2,367-bp open reading frame is shown contained within the minimum complementing BglII/BamHI fragment. A deletion construct replacing 92% of the open reading frame with the HIS3 gene is schematized. *Bg*, BglII; *C*, ClaI; *X*, XhoI; *Bs*, BstBI; *P*, PvuII; *B*, BamHI. (*B*) SEY6210 (wild-type) and BWY6 (*dim1-Δ*) with or without complementing pDIM1 plasmid were grown on YPD plates at 30°C or 37°C for 3 d.

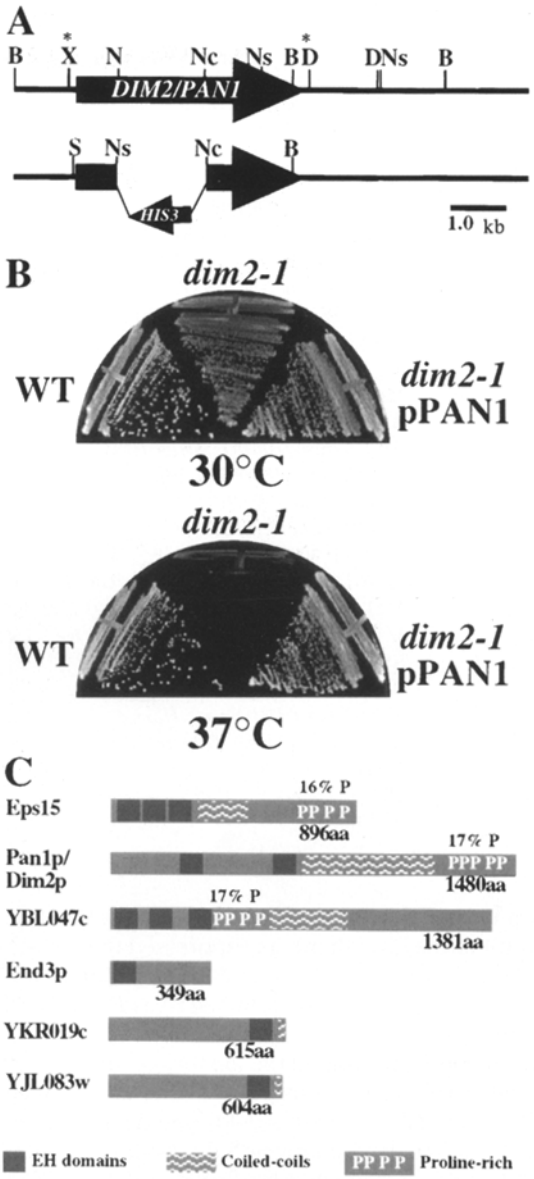

Figure 6. Analysis of the *PAN1/DIM2* gene. (*A*) A 12-kb genomic fragment was isolated that complemented the growth defect of BWY10 (*dim2-1*) cells. The 4,440-bp open reading frame is shown contained within the minimum complementing XmnI/DraI fragment (denoted by *). A deletion construct removing the central one third of the open reading frame is schematized. *B*, BamHI; *X*, XmnI; *Ns*, NsiI; *S*, SalI; *Nc*, NcoI; *D*, DraI. (*B*) SEY6210 (wild-type) and BWY16 (*dim2-1*) with or without complementing pPAN1 plasmid were grown on YPD plates at 30°C or 37°C for 3 d. (*C*) Comparison of the domain structures of yeast proteins that contain EH domains to the mammalian eps15 protein. *Gray boxes*, EH domains; *hatched boxes*, regions rich in heptad repeats, *PPPP*, proline-rich domains.

type (Fig. 2). The growth defect and *dim* phenotypes are rescued in *she4-Δ* cells that harbor a complementing plasmid (Figs. 2 and 5 *B*).

The *DIM2* gene was isolated by complementation of the growth defect in *dim2-1* cells at 38°C. Two distinct library plasmids that rescued the growth defect were analyzed by restriction mapping and contained a common region of overlapping sequence. The largest clone, which fully complemented the mutant, is schematized in Fig. 6 *A*. Several regions of the clone were sequenced. Comparison with the database revealed identity to a previously characterized essential gene of unknown function, *PAN1* (Sachs and Deardorff, 1992; Boeck et al., 1996), and also to the chromosome IX open reading frame YIR006C (Voss et al., 1995). *PAN1* was originally thought to encode a poly-A–specific nuclease, but was recently reported to be a contaminant in the purification of Pan2p, the true nuclease (Boeck et al., 1996). *PAN1* has also been isolated recently in other screens for mitochondrial protein–targeting mutants (Zoladek et al., 1995) and rapid-death mutants with *cdc28-4* (Tang and Cai, 1996). Five regions of discrepancy between *PAN1* and open reading frame YIR006C have been reported. Sequencing of these regions in our library plasmid indicated identity with the open reading frame YIR006C sequence, which predicts a 1,480–amino acid protein. The sequence variations may be the result of strain differences, recombination events, or sequencing errors. The temperature sensitivity and *dim* phenotype of the *dim2-1* cells was rescued by a plasmid containing the minimum comple-

Table I. Genotypes of Yeast Strains

SEY6210	*MATα ura3-52 his3-Δ200 trp1-Δ901 leu2-3, 112 lys2-801 suc2-Δ9*	(Robinson et al., 1988)
SEY6211	*MATa ura3-52 his3-Δ200 trp1-Δ901 leu2-3, 112 ade2-101 suc2-Δ9*	(Robinson et al., 1988)
SEY6210.5	*MATα/MATa ura3-52/ura3-52 lys2-801 ade2-101 trp1-Δ901/trp1-Δ901 leu2-3, 112/leu2-3, 112 suc2-Δ9/suc2-Δ9*	(Herman and Emr, 1990)
RH268-1C	*MATa leu2 ura3 his4 bar1-1 end4-1*	(Raths et al., 1993)
DBY1691	*MATa his4-619 act1-1*	(Novick and Botstein, 1985)
DBY1692	*MATα his4-619 act1-1*	(Novick and Botstein, 1985)
GPY 1100α	*MATα leu2-3, 112 ura3-52 his4-519 trp1 can1*	(Tan et al., 1993)
GPY 418	*MATα leu2-3, 112 ura3-52 his4-519 trp1 can1 chc1-521*	(Tan et al., 1993)
YAS1114	*MATα ade2 his3 leu2 ura3 trp1 PAN1::HIS3 pPAN1-URA3-CEN*	A. Sachs
YAS1115	*MATα ade2 his3 leu2 ura3 trp1 PAN1::HIS3 ppan1-3-URA3-CEN*	A. Sachs
KMY1004α	*SEY6210 vma4-Δ::URA3*	D. Klionsky
BWY1	*MATa ura3-52 his3-Δ200 trp1-Δ901 leu2-3, 112 lys2-801 suc2-Δ9 she4-1*	This study
BWY2	*MATα ura3-52 his3-Δ200 trp1-Δ901 leu2-3, 112 lys2-801 suc2-Δ9 she4-1*	This study
BWY3	BWY1/BWY2 (diploid)	This study
BWY4	BWY3 *she4-1/she4-1::SHE4-HIS3*	This study
BWY5	SEY6210.5 *SHE4/SHE4::HIS3*	This study
BWY6	SEY6210 *she4-Δ::HIS3*	This study
BWY7	SEY6211 *she4-Δ::HIS3*	This study
BWY8	BWY5/BWY6 (diploid)	This study
BWY9	SEY6211 *she4-Δ::HIS3 bar1-Δ::URA3*	This study
BWY10	*MATa ura 3-52 his3-Δ200 trp1-Δ901 leu2-3, 112 lys2-801 suc2-Δ9 pan1-20*	This study
BWY11	*MATα ura3-52 his3-Δ200 trp1-Δ901 leu2-3, 112 lys2-801 suc2-Δ9 pan1-20*	This study
BWY12	BWY9/BWY10 (diploid)	This study
BWY13	BWY12 *pan1-20/pan1-20::PAN1-HIS3*	This study
BWY14	SEY6210.5 *PAN1/PAN1::HIS3*	This study
BWY15	*MATa ura3-52 his3-Δ200 trp1-Δ901 leu2-3, 112 lys2-801 suc2-Δ9 bar1-1 pan1-20*	This study
BWY16	*MATα ura3-52 his3-Δ200 trp1-Δ901 leu2-3, 112 lys2-801 suc2-Δ9 pan1-20*	This study
BWY17	*SEY6211 bar1-Δ::URA3*	This study

menting XmnI-DraI fragment (Figs. 2 and 6 *B*). Addition of 1 M sorbitol to the growth media suppressed the growth defect at 38°C both for *she4-Δ* and *dim2-1* (data not shown). Hereafter, *DIM2* will be referred to as *PAN1*, and the *dim2-1* allele as *pan1-20.*

Integrative mapping confirmed the identity of the *pan1-20* locus with the *PAN1* gene. Disruption of the *PAN1* gene with the *HIS3* gene (Fig. 6 *A*) in a wild-type diploid strain followed by tetrad analysis confirmed the essential nature of the *PAN1* gene, as reported by Sachs and Deardorff (1992). Dissection of the tetrads onto 1 M sorbitol plates did not permit germination of the spores (data not shown).

Interestingly, Pan1p was found to contain two EH (eps15 homology) domains with 30–40% identity to similar domains in eps15 (Fazioli et al., 1993; Wong et al., 1995). In addition to containing EH domains, the two proteins also share a similar overall structure: both proteins include EH domains at their amino termini, central portions with a high probability of forming coiled coils, and carboxy-terminal, proline-rich domains with hallmarks of SH3-binding proteins (Wong et al., 1995; Fig. 6 *C* in this paper). Other yeast proteins containing EH domains include End3p (Benedetti et al., 1994), as well as the *S. cerevisiae* open reading frames YBL047c, YKR019c, and YJL083w. Comparison of the overall domain structure of mammalian eps15 with YBL047c and Pan1p (Fig. 6 *C*) suggests that eps15 is more similar to YBL047c than it is to Pan1p. We constructed a deletion of YBL047c, which has no assigned function, and have found that the deletion strain is viable and no obvious growth defects have been detected (our unpublished data).

SHE4 and PAN1 Interact with Other Genes Involved in Endocytosis

Munn and Riezman (1994) recently described a screen in which endocytosis mutants were isolated by selecting for mutants that exhibited synthetic lethality in combination with vacuolar ATPase (v-ATPase) mutants. This screen was based on the fact that v-ATPase mutants require acidic media for viability and the supposition that viability is dependent on vacuole acidification via endocytosis of protons (Nelson and Nelson, 1990). We asked whether the *dim* mutants also fell into this class of endocytosis mutants. *VMA4* encodes a subunit of the v-ATPase (Ho et al.,

Table II. Growth Phenotypes of Double Mutants

	act1-1		*end4-1*	*vma4-Δ*
	26°C	30°C	20°C	20°C
she4-Δ	+	+/−	−−/+	−−/+
pan1-20	+	+/−	+/−	−

	chc1^{ts}		*pan1-3*	
	30°C	35°C	30°C	35°C
she4-Δ	++	−	+	−

Strains that contained two mutant alleles were constructed, and their growth phenotypes at various temperatures were tested. ++, wild-type growth; +, growth that is slower than wild type; +/−, very slow growth; −−/+, almost no growth; and −, complete lethality. All strains were tested on rich YPD plates, except the strains containing *vma4-Δ* alleles, which were grown on MES-buffered YPD plates, pH 5.5. In each case, the single mutants grew nearly as well as the wild type at all temperatures reported in this table.

1993), and a *vma4-Δ* strain is deficient in v-ATPase function. *she4-Δ vma4-Δ* and *pan1-20 vma4-Δ* heterozygous diploids were sporulated and dissected, and synthetic lethality was observed in spores that were deduced to harbor both mutations, consistent with the endocytosis defects observed in the *dim* mutants (Table II).

Synthetic growth defects often are used as an argument to place gene products the same or parallel pathways. We observed synthetic growth defects in strains harboring both *she4-Δ* and the temperature-sensitive endocytosis mutant alleles *end4-1* (Raths et al., 1993) or *act1-1* (Shortle et al., 1984; Novick and Botstein, 1985; Munn et al., 1995). Also, *pan1-20* in combination with *end4-1* or *act1-1* yielded strains that grew more poorly than strains containing single mutations (Table II). Furthermore, synthetic growth defects were observed in double mutants between *she4-Δ* and *pan1-3* (Sachs and Deardorff, 1992), and also with *she4-Δ* and *chc-ts* (Tan et al., 1993; Table II in this paper). These data are indicative of a role for the *SHE4* and *PAN1* gene products in endocytosis (also see Discussion).

Actin Cytoskeleton Structure Is Altered in she4-Δ and pan1-20 Cells

The actin cytoskeleton is intimately involved in the process of endocytosis in yeast (Kubler and Riezman, 1993; Munn et al., 1995). Actin localization in yeast cells changes as a function of cell cycle progression, and patches of filamentous actin (actin cortical dots) at the plasma membrane coincide with sites of synthesis of new cell wall material in budding cells and with secretion of a-agglutinin in shmooing (mating) cells (Adams and Pringle, 1984; Kilmartin and Adams, 1984). The normal polarized localization of actin is disrupted in many previously described endocytosis mutants (Benedetti et al., 1994; Munn et al., 1995), so we examined the structure and polarity of the actin cytoskeleton in the *she4-Δ* and *pan1-20* cells.

Wild-type, *she4-Δ*, and *pan1-20* diploid cells were fixed and then incubated with rhodamine-phalloidin to label filamentous actin. In *she4-Δ* cells, we observed a loss of polarity of actin localization at both 26°C (Fig. 7 *A*) and 38°C (data not shown). The cells also adopted a round morphology at all temperatures, similar to that seen with *act1-1* mutant cells (Novick and Botstein, 1985), and consistent with a loss of polarized secretion and a switch to isotropic growth. Normal elongated cell morphology and polarity of actin cortical spots were restored in a *she4-Δ* strain harboring a complementing plasmid (Fig. 7 *A*).

pan1-20 diploid cells revealed slightly disrupted actin polarity at 26°C, with a few more cortical spots found in the mother cells relative to wild-type cells (data not shown), and the cells were rounder than wild-type cells, consistent with the mislocalization of actin spots. After incubation at 38°C for 2.5 h, the morphology of the actin cytoskeleton became markedly perturbed: thick, curved actin bundles appeared to be adjacent to the cell periphery, and polarity of the cortical spots was lost (Fig. 7 *B*). Mislocalization of actin in a *pan1* allele was also recently reported by Tang and Cai (Tang and Cai, 1996). In addition, actin structures did not display the wild type double band of cortical dots at the neck during cytokinesis and instead adopted a filamentous appearance with a larger amount of actin directed toward the smaller (presumably daughter) cell. Actin polarity and cell shape were restored to a wild-type appearance when *pan1-20* cells harbored a complementing plasmid (Fig. 7 *B*).

Budding yeast exhibit stereotypic patterns of bud site selection: haploid cells bud in an axial pattern in which the next budding event occurs adjacent to the previous one, whereas diploid cells can bud from either pole of their el-

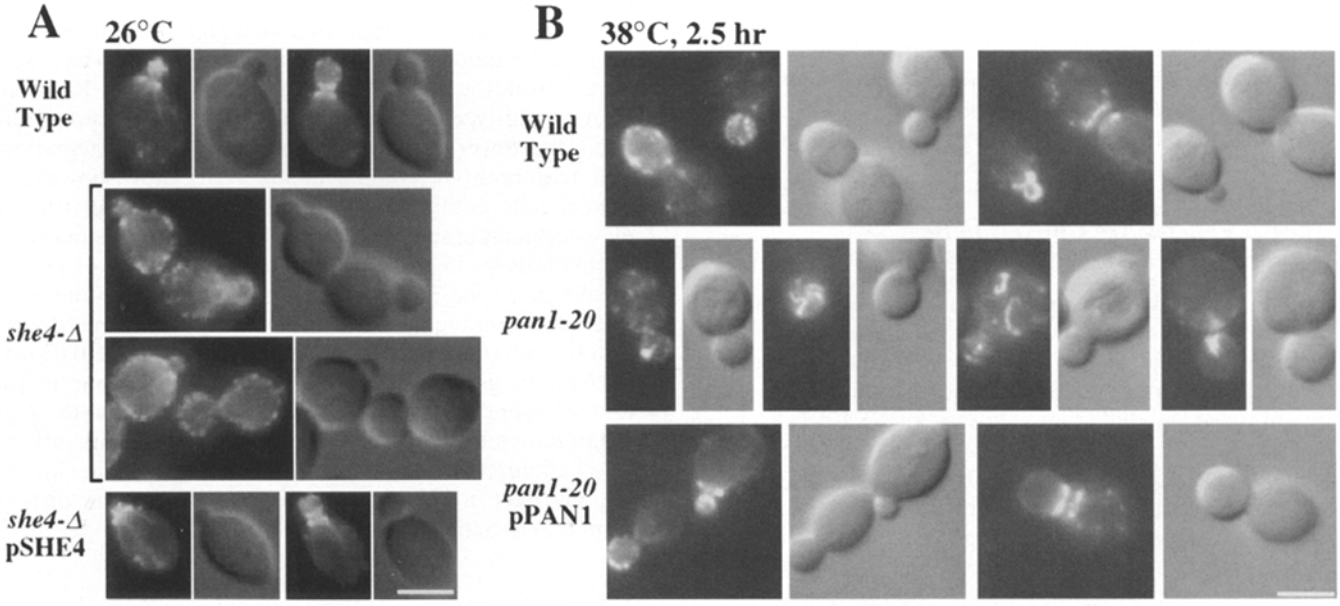

Figure 7. Localization of filamentous actin. (*A*) Diploid SEY6210.5 (wild-type) and BWY8 (*she4-Δ*) with or without complementing plasmid were grown at 26°C, fixed with formaldehyde, and labeled with rhodamine-conjugated phalloidin to visualize filamentous actin. (*B*) Diploid SEY6210.5 (wild-type) and BWY12 (*pan1-20*) with or without complementing plasmid were grown at 26°C, shifted to 38°C for 2.5 h before fixation with formaldehyde, and labeled with rhodamine-conjugated phalloidin to visualize filamentous actin. Bar, 5 μm.

lipsoidal shape (Chant and Pringle, 1995). Haploid *she4-Δ* and *pan1-20* cells were capable of normal axial budding as seen in wild-type cells; however, in diploid *she4-Δ* and *pan1-20* cells, the budding pattern became random (data not shown). The same diploid-specific alterations in bud site selection are also observed in other endocytosis mutants such as *end3* (Benedetti et al., 1994), *rvs161/end6* (Sivadon et al., 1995), and *rvs167* (Bauer et al., 1993).

Ultrastructural Analysis of she4-Δ and pan1-20 Cells Reveals Vesicles and Tubulovesicular Membranes

When the *dim* mutants are examined with the light microscope for FM4-64 internalization and localization of filamentous actin, defects that may correlate with morphological aberrations are observed. EM was performed to examine more closely the structure of these mutants. In the *she4-Δ* cells, EM revealed the presence of 100-nm vesicles in the cytoplasm at both 26°C (Fig. 8, *B* and *C*) and 38°C (Fig. 8, *D–G*), whereas in wild-type cells, such structures are rarely detected (Fig. 8 *A*). Additional tubulovesicular compartments reminiscent of early endosomes in mammalian cells (Helenius et al., 1983), as well as 40–50-nm vesicles, appeared upon incubation at 38°C. These structures may correspond to the punctate staining that is observed in FM4-64 labeling after a temperature shift, and they may represent endocytic intermediate compartments. While fewer 50- and 100-nm vesicles were observed, similar endosomal-like structures were also seen in the *pan1-20* cells after incubation at 38°C, whereas they were absent in *pan1-20* cells containing a complementing plasmid (data not shown).

In many cases, the 100-nm vesicles observed in the *she4-Δ* cells at 26°C appeared to have associated coats (Fig. 8 *C*). These vesicles are unlikely to correspond to classical post-Golgi secretory vesicles because sorting and processing of the vacuolar hydrolase carboxypeptidase Y (Stevens et al., 1982) and secretion of the heat shock protein Hsp150p (Russo et al., 1992) did not differ from wild-type cells at 26°C or 30°C (data not shown). A partial kinetic defect in secretion of Hsp150p and the periplasmic enzyme invertase (Gascon et al., 1968) was observed at 38°C; however, this may be caused by lack of growth at 38°C (data not shown).

she4-Δ Vesicles Are Unlikely to Be Clathrin-coated Vesicles

Given the established role for clathrin heavy chain in endocytosis (Tan et al., 1993), we tested if the 100-nm coated vesicles observed in the *she4-Δ* cells were clathrin coated. After the protocol of Mueller and Branton (1984), light membranes isolated from wild-type or *she4-Δ* cells grown at 30°C were fractionated by size on an S-1000 Sephacryl column (Fig. 9, *A* and *B*). A 280-nm absorbance peak was observed in fractions 33–38 from *she4-Δ* membranes that was not observed from wild-type membranes, suggesting that this peak might correspond to the observed vesicles. To determine the elution position of clathrin-coated vesicles, every fifth fraction was assayed by immunoblotting with antibodies to the heavy chain of the clathrin triskelion (Chc1p). The peak of Chc1p elution was not coincident with the large absorbance peak (Fig. 9 *B*). For further analysis, membranes from fractions 36–37 and 45–50 were concentrated and prepared for examination by conventional EM (Fig. 9, *C* and *D*). Fractions 36–37 contained a fairly homogeneous population of 100-nm vesicles consistent with the size of vesicles observed in sections of spheroplasted cells (Fig. 8, *B* and *C*). In contrast, fractions coincident with clathrin immunoreactivity contained a heterogeneous population of vesicles, including many with coats exhibiting a classic clathrin cagelike coat (Fig. 9 *D*, *arrowheads*). Thus it is unlikely that the vesicles in the *she4-Δ* cells represent clathrin-coated vesicles, although they could be vesicles that have lost their coats, vesicles coated with a nonclathrin coat, or endocytic vesicles of an unknown origin.

Cationized Ferritin Internalization Reveals Endocytic Structures at the Plasma Membrane

To examine the structure and morphology of the endocytic pathway at the ultrastructural level, internalization of cationized ferritin was assayed. This is a commonly used method for following the endocytic pathway in mammalian cells (Ottosen et al., 1980; Herzog and Farquhar, 1983), but had not yet been used in yeast. Yeast cells were spheroplasted in an osmotically supported environment and preincubated at permissive or nonpermissive temperatures for 30–60 min, followed by incubation with cationized ferritin for 30 min. Ferritin accumulation was observed in numerous plasma membrane invaginations in *she4-Δ* cells at 30°C (Fig. 10, *A* and *B*) and 38°C (Fig. 10 *C*) and in *pan1-3* (Fig. 10 *D*) and *end4-1* cells at 38°C (data not shown). In wild-type cells, roughly half as many invaginations (0.46 invaginations per micrometer of plasma membrane, wild type; 0.81 invaginations per micrometer of plasma membrane, *she4-Δ*) that were significantly shallower (0.08 +/− 0.03 μm, wild type; 0.16 +/− 0.04 μm, *she4-Δ*) and that only rarely contained cationized ferritin labeling were observed. In addition, in *she4-Δ* cells at 30°C, membranous compartments within the cell that may represent endocytic intermediates that appear to have separated from the cell surface were observed (Fig. 10 *B*). As seen in wild-type cells, *end4-1* at a permissive temperature exhibited fewer, rarely labeled membrane invaginations and membranous compartments (data not shown). In *pan1-3* cells, compared to the isogenic wild-type strain at elevated temperature, we observed five times as many invaginations (0.55 invaginations per micrometer of plasma membrane, *pan1-3*; 0.11 invaginations per micrometer of plasma membrane, *PAN1*) that extended >10 times deeper into the cell (0.43 +/− 0.15 μm, *pan1-3*; 0.03 +/− 0.02 μm, *PAN1*). In general, the membrane invaginations in the mutants were deeper and often more elaborate at the high temperature than at the lower, permissive temperatures. The cationized ferritin–labeled plasma membrane invaginations have a morphology that appears to be distinct from that of actin cortical dots (Mulholland et al., 1994).

Discussion

The *dim* mutants described here were identified in a novel screen for mutants defective in bulk lipid endocytosis. Two mutants (*dim1/she4*, *dim2/pan1*) were characterized in de-

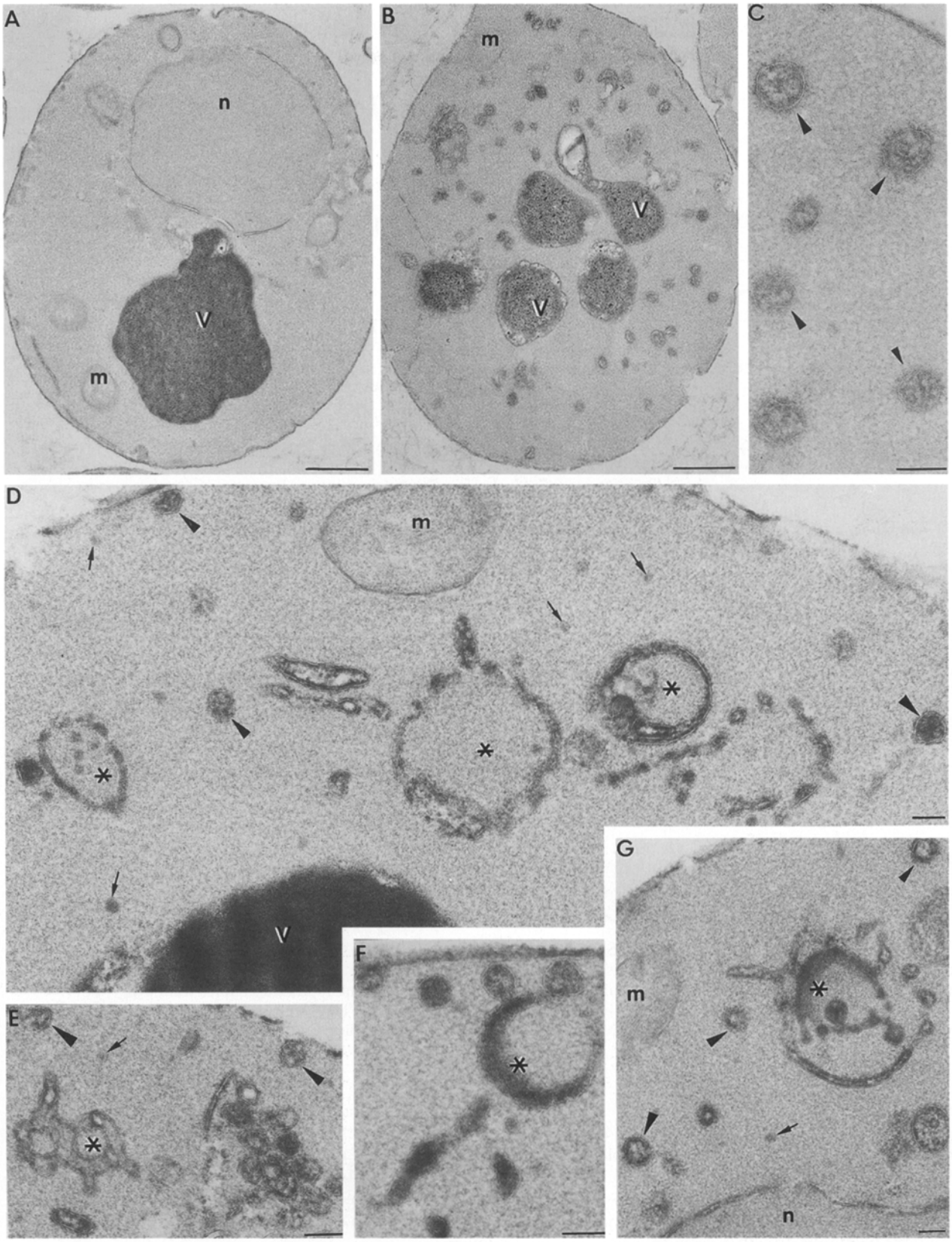

Figure 8. EM of wild-type and *she4-Δ* cells. (*A*) SEY6210 (wild-type) and (*B* and *C*) BWY6 (*she4-Δ*) cells were grown at 26°C, and (*D–G*) a portion shifted to 38°C for 90 min before glutaraldehyde fixation. *M*, mitochondria; *N*, nucleus; *V*, vacuole; *arrowheads*, 100-nm vesicles; *small arrows*, 40–50-nm vesicles; *asterisks*, tubulovesicular compartments. Bar in *A* and *B*, 0.5 μm; *C–G*, 0.1 μm.

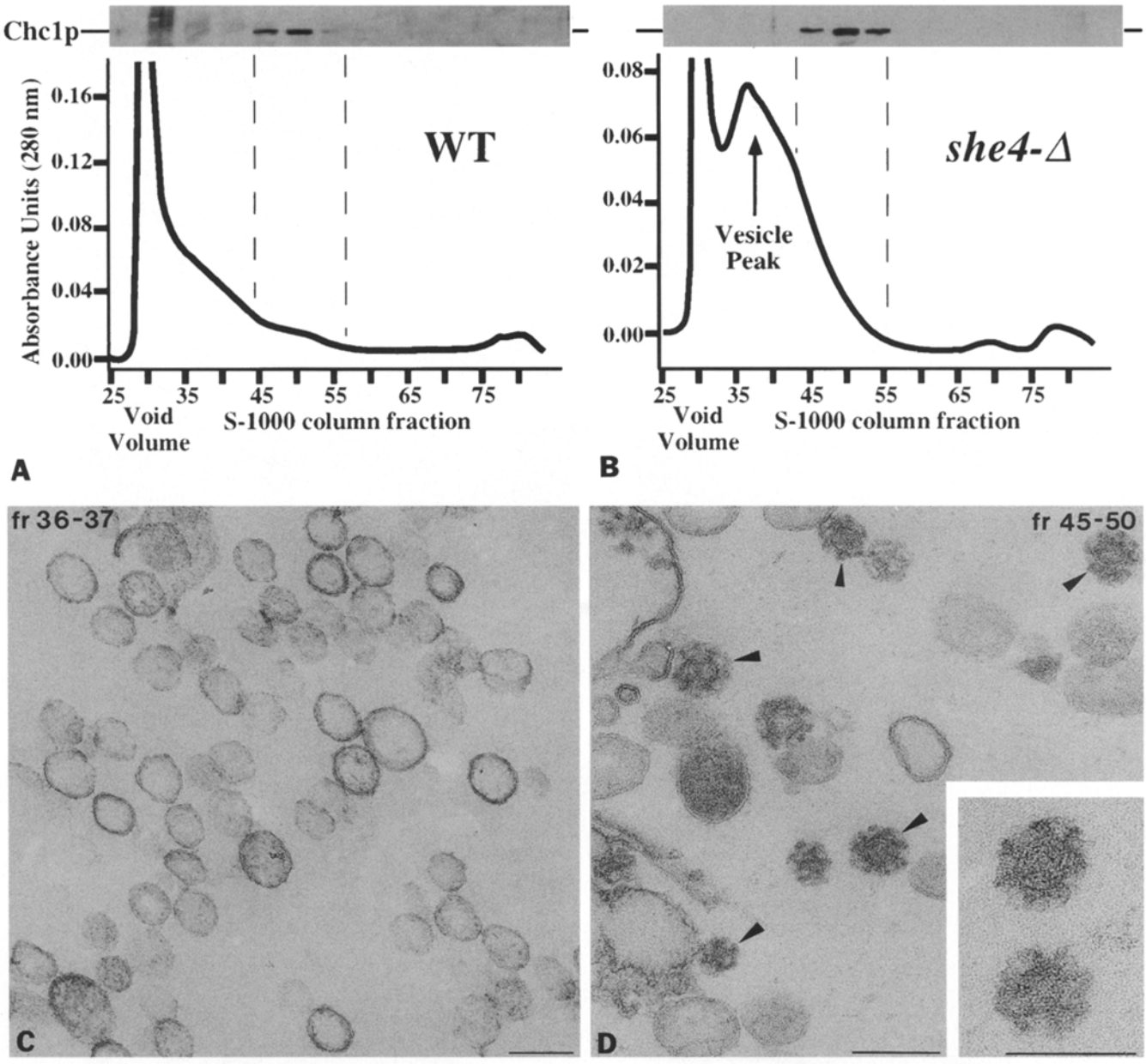

Figure 9. Purification of clathrin-coated vesicles. (*A*) SEY6210 (wild-type) and (*B*) BWY6 (she4-Δ) cells were grown at 30°C, spheroplasted, osmotically lysed, and light membranes were isolated by centrifugation. The pelleted membranes were resuspended, separated by size on a Sephacryl S-1000 column, and the absorbance at 280 nm was monitored. Immunoblotted samples from every fifth fraction were assayed for content of clathrin heavy chain. (*C*) Membranes from fractions 36 and 37 and (*D*) fractions 45–50 purified from BWY6 (*she4-Δ*) cells were fixed, pelleted, and examined by EM. *Arrowheads*, coated vesicle profiles. Bar, 0.1 μm.

tail. These two temperature-sensitive *dim* mutants exhibit defects in internalization of the lipophilic dye FM4-64, they display reduced kinetics of α-factor internalization as compared to wild-type cells, and they also exhibit altered actin localization. Previously characterized mutants in the early steps of endocytosis share these general phenotypes with the *dim* mutants. Synthetic growth defects between the *dim* mutants and other endocytosis mutants are consistent with these gene products acting at similar stages in endocytosis. Both *dim* mutants also accumulated vesicles and aberrant membranous compartments with morphology reminiscent of mammalian early endosomes. In contrast, neither mutant yielded significant defects in secretory function. This new screening technique has thus allowed the identification of new genes involved in endocytosis. In addition, the usefulness of FM4-64–based FACS® screening for mutants in yeast was also recently demonstrated by Wang et al. (1996) in a search for mutants defective in vacuolar inheritance.

The yeast actin cytoskeleton is known to play an important role in endocytosis. Endocytosis mutants almost invariably exhibit disorganized actin cytoskeletons; and not surprisingly, many mutants with a perturbed actin cytoskeleton exhibit defects in endocytosis (Kubler and Riez-

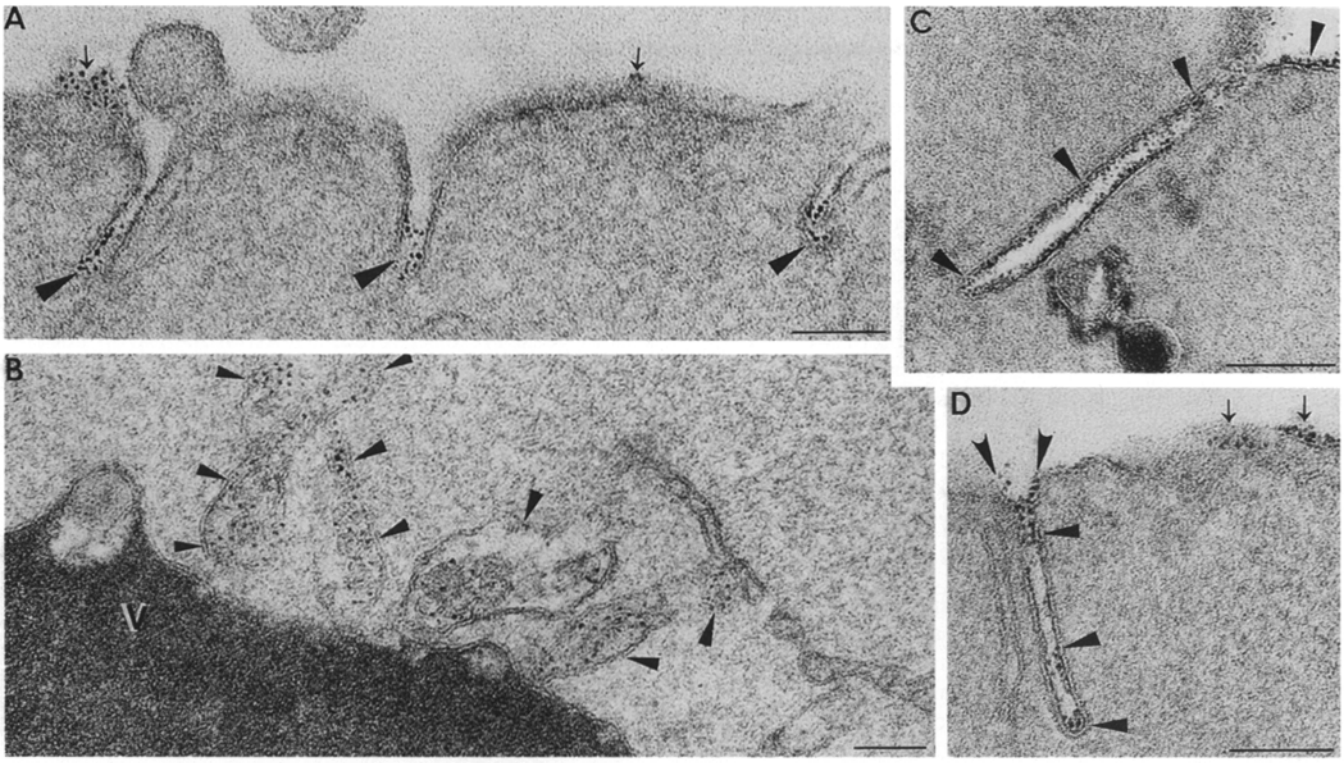

Figure 10. Cationized ferritin internalization in *dim* mutants. (*A–C*) BWY6 (*she4-Δ*) and (*D*) YAS1115 (*pan1-3*) cells were spheroplasted in 1.2 M sorbitol for osmotic support and preincubated at 30°C (*A* and *B*) or 38°C (*C* and *D*) for 30 min, followed by incubation with 1 mg/ml cationized ferritin (*arrowheads*) for 30 min. The cells were then fixed and examined by EM. *Arrowheads*, internalized cationized ferritin; *small arrows*, surface-bound ferritin; *V*, vacuole. Bar, 0.1 μm.

man, 1993; Munn et al., 1995). In yeast, the actin cytoskeleton is comprised of fine cytoplasmic cables and cortical actin dots that correlate with sites of secretion and cell growth (Adams and Pringle, 1984). The identity of the thick actin bundles observed in the *pan1-20* cells at 38°C and their possible relationship to actin cortical dots or other actin-based complexes remains to be clarified. The structure of actin cortical dots, which has been described as a fingerlike invagination of plasma membrane surrounded by actin filaments (Mulholland et al., 1994), and perhaps the structure of other membrane invaginations are suggestive of their role as a reservoir of membrane that can be used for secretion, endocytosis, and responses to osmotic changes. The observation that *dim* and *end* mutant cells exhibit an enlarged and rounded morphology suggests that the restricted sites for exocytosis and/or the normal balance between exocytosis and endocytosis are perturbed. It has been proposed that these two processes are coordinated through the homeostasis of membrane tension (Sheetz and Dai, 1996).

The actin cytoskeleton is important for establishing the distinction between mother and daughter cells during budding. This developmental asymmetry is exemplified by the process of mating-type switching: only mother cells are capable of mating-type switching in wild-type strains (Nasmyth, 1993), while *she* mutants exhibit defects in this asymmetry and in mating-type switching (Jansen et al., 1996). The fact that mutations in *SHE4/DIM1* cause defects both in mating-type switching and in endocytosis (Figs. 2–4) may reflect the importance of the actin cytoskeleton in each of these processes. In addition, the identification of *SHE1* as *MYO4* suggests a role for actin/myosin interactions in directing traffic from the mother cell to the daughter cell (Jansen et al., 1996; see also Johnston et al., 1991; Govindan et al., 1995). It is possible that the block of mating-type switching in the *she4* mutant is an indirect consequence of the mislocalization of actin cables and cortical spots. Actin polarization may be required for the proper asymmetric localization of factors that regulate mating-type switching (Jansen et al., 1996).

While presently there are no known homologues to She4p, there are several proteins in yeast and mammalian cells with very significant homology to Pan1p/Dim2p, including eps15 (Wong et al., 1995). The mammalian protein eps15 was first discovered as a phosphorylated substrate of the EGF receptor tyrosine kinase (Fazioli et al., 1993). eps15 is comprised of three domains: three imperfect tandem repeats in the amino terminus (EH domains), a central domain rich in heptad repeats that are predicted to form coiled coils, and a carboxy-terminal proline-rich region, a portion of which has been shown to interact with the SH3 domains contained within the signaling molecule crk (Schumacher et al., 1995). The carboxy terminus of eps15 also contains a 72–amino acid domain that is distinct from the crk-binding motif, which has been demonstrated to interact constitutively with the plasma membrane adaptor complex AP2 (Benmerah et al., 1995, 1996). The interaction between eps15 and AP2 is intriguing because AP2 interacts with clathrin to promote clathrin-coated pit assembly at the plasma membrane (Smythe et al., 1992), thus

providing a connection between eps15 and endocytosis. Pan1p and the yeast YBL047c protein share extensive structural similarity with eps15, each containing coiled-coil and proline-rich domains (Fig. 6). The proline-rich domains of Pan1p and the YBL047c protein are likely to interact with SH3 domain–containing proteins (Ren et al., 1993; Yu et al., 1994); several candidates include proteins associated with the actin cytoskeleton (e.g., Abp1p [Drubin et al., 1990] and Sla1p [Holtzman et al., 1993]) and proteins implicated in endocytosis (e.g., Rvs167p [Bauer et al., 1993; Munn et al., 1995] and Myo3p [Goodson and Spudich, 1995; Geli and Riezman, 1996]). An additional correlation between eps15 and endocytosis is provided by the presence of EH domains in the yeast proteins End3p and Pan1p (Benedetti et al., 1994; Wong et al., 1995). EH domain–containing proteins have been proposed to function in endocytosis or at other sites of membrane trafficking (Seaman et al., 1996). Clearly, an area of great interest is the identification of other molecules that interact with each of these structural motifs.

Endocytosis in yeast has been particularly difficult to study morphologically, partly because of the uncharacterized structure of the endosomal membrane system in this organism. It is interesting to speculate on the identity of the tubulovesicular structures that accumulate in the *dim* mutants. These structures accumulated after shifts to elevated temperatures (Fig. 8), correlating well with the appearance of punctate staining in FM4-64–labeling experiments (Fig. 2). Further studies will be necessary to equate these two compartments unambiguously. It is intriguing to compare these structures with the tubulovesicular early endosomes that are observed in mammalian cells (Helenius et al., 1983). Our results with cationized ferritin provide a view of early internalization structures in yeast (Fig. 10). However, additional high resolution probes and techniques will be required to define each of the endocytic intermediates in yeast.

Several lines of evidence in both yeast and mammalian cells suggest the presence of two or more endocytic pathways (Sandvig and van Deurs, 1994). It has been shown in mammalian cells that different receptors rely upon distinct pathways for their endocytosis: the EGF receptor enters cells via clathrin-coated pits (Willingham and Pastan, 1982), while the folate receptor is internalized through a clathrin-independent pathway (Rothberg et al., 1990). It has also been shown that mammalian cells disrupted in the dynamin/clathrin–coated pit pathway upregulate an alternate endocytic pathway (Damke et al., 1995). In yeast, *chc1-Δ* strains are viable and endocytose FM4-64 (data not shown) and α-factor receptor (Payne et al., 1987, 1988), suggesting that two or more endocytic pathways in yeast may also exist. In addition, a *dim* phenotype was observed when the *end3-1* and *end4-1* strains were tested for FM4-64 internalization (data not shown). This suggests that a block in internalization of mating pheromone receptor is not sufficient to completely block all flow from the plasma membrane into the cell. The synthetic growth defects we observed in double endocytosis mutants are also consistent with a multiple endocytic pathway model. Additionally, because *act1-1* displays both endocytic and late secretory defects, it remains possible that the synthetic growth defects observed in *act1-1/dim* mutants are in part caused by perturbations of secretory function in the *dim* mutants. *chc1-ts* mutants also display multiple membrane trafficking defects, including deficiencies in vacuolar protein sorting and endocytosis. However, since the vacuolar protein sorting pathway is normal in *dim* mutants, the synthetic defect observed in *chc-ts/dim* double mutants is a likely result of combined endocytosis deficits. Finally, synthetic defects between secretory and endocytic mutants in general might be expected if these two processes are tightly coupled.

As increasing numbers of proteins that mediate endocytosis in yeast are discovered, a need arises for an understanding of the precise functions of each of these proteins, how they are regulated, and how they interact with one another. Future studies will include the use of this FM4-64 screening strategy for the identification of additional endocytosis mutants. Genetic and two-hybrid screens will shed light on interacting partners that might establish pathways in endocytic membrane traffic. In vitro assays should allow for the purification of activities that are necessary for internalization and subsequent stages of membrane traffic. Through the use of these screens and other approaches, it should be possible to identify biologically significant interactions among relevant gene products, and to decipher molecular mechanisms for the control of endocytosis in eukaryotic cells.

We are especially grateful for the technical and scientific advice provided by Marilyn Farquhar. We also would like to thank the members of the Emr lab for many helpful discussions, particularly Erin Gaynor, Chris Burd, and Matthew Seaman for critical reading of the manuscript, as well as Peggy Mustol for expert technical assistance. We also thank Tom Vida, Alan Sachs, Julie Deardorff, Howard Riezman, David Botstein, Greg Payne, and Dan Klionsky for providing strains, constructs, antibodies, and helpful information; Philip Hieter for the *LEU2-CEN* genomic library; and Celeste Wilcox for assistance with the α-factor uptake experiments.

This work is dedicated to the memory of Linda Rogers Morreale. This work was supported by grants from the National Institutes of Health (GM32703 and CA58689 to S.D. Emr). B. Wendland is supported as an Associate of the Howard Hughes Medical Institute, and S.D. Emr is supported as an Investigator of the Howard Hughes Medical Institute.

Received for publication 23 August 1996 and in revised form 30 September 1996.

References

Adams, A.E., and J.R. Pringle. 1984. Relationship of actin and tubulin distribution to bud growth in wild-type and morphogenetic-mutant *Saccharomyces cerevisiae*. *J. Cell Biol.* 98:934–945.

Anderson, R.G., M.S. Brown, and J.L. Goldstein. 1977. Role of the coated endocytic vesicle in the uptake of receptor-bound low density lipoprotein in human fibroblasts. *Cell.* 10:351–364.

Bauer, F., M. Urdaci, M. Aigle, and M. Crouzet. 1993. Alteration of a yeast SH3 protein leads to conditional viability with defects in cytoskeletal and budding patterns. *Mol. Cell. Biol.* 13:5070–5084.

Benedetti, H., S. Raths, F. Crausaz, and H. Riezman. 1994. The END3 gene encodes a protein that is required for the internalization step of endocytosis and for actin cytoskeleton organization in yeast. *Mol. Biol. Cell.* 5:1023–1037.

Benmerah, A., B. Begue, A. Dautry-Varsat, and N. Cerf-Bensussan. 1996. The ear of alpha-adaptin interacts with the COOH-terminal domain of the Eps15 protein. *J. Biol. Chem.* 271:12111–12116.

Benmerah, A., J. Gagnon, B. Begue, B. Megarbane, A. Dautry-Varsat, and N. Cerf-Bensussan. 1995. The tyrosine kinase substrate eps15 is constitutively associated with the plasma membrane adaptor AP-2. *J. Cell Biol.* 131:1831–1838.

Boeck, R., S. Tarun, Jr., M. Rieger, J.A. Deardorff, S. Muller-Auer, and A.B. Sachs. 1996. The yeast Pan2 protein is required for poly(A)-binding protein-stimulated poly(A)-nuclease activity. *J. Biol. Chem.* 271:432–438.

Bullock, W.O., J.M. Fernandez, and J.M. Short. 1987. Biotechniques. 5:376–379.

Cain, C.C., R.B. Wilson, and R.F. Murphy. 1991. Isolation by fluorescence-activated cell sorting of Chinese hamster ovary cell lines with pleiotropic, temperature-conditional defects in receptor recycling. *J. Biol. Chem.* 266:11746–11752.

Callebaut, I., J.M. Renoir, M.C. Lebeau, N. Massol, A. Burny, E.E. Baulieu, and J.P. Mornon. 1992. An immunophilin that binds M(r) 90,000 heat shock protein: main structural features of a mammalian p59 protein. *Proc. Natl. Acad. Sci. USA.* 89:6270–6274.

Chant, J., and J.R. Pringle. 1995. Patterns of bud-site selection in the yeast *Saccharomyces cerevisiae. J. Cell Biol.* 129:751–765.

Damke, H., T. Baba, A.M. van der Bliek, and S.L. Schmid. 1995. Clathrin-independent pinocytosis is induced in cells overexpressing a temperature-sensitive mutant of dynamin. *J. Cell Biol.* 131:69–80.

Drubin, D.G., J. Mulholland, Z.M. Zhu, and D. Botstein. 1990. Homology of a yeast actin-binding protein to signal transduction proteins and myosin-I. *Nature (Lond.).* 343:288–290.

Dulic, V., M. Egerton, I. Elguindi, S. Raths, B. Singer, and H. Riezman. 1991. Yeast endocytosis assays. *Methods Enzymol.* 194:697–710.

Fazioli, F., L. Minichiello, B. Matoskova, W.T. Wong, and P.P. Di Fiore. 1993. eps15, a novel tyrosine kinase substrate, exhibits transforming activity. *Mol. Cell Biol.* 13:5814–5828.

Gammie, A.E., L.J. Kurihara, R.B. Vallee, and M.D. Rose. 1995. DNM1, a dynamin-related gene, participates in endosomal trafficking in yeast. *J. Cell Biol.* 130:553–566.

Gascon, S., P. Neumann, and J.O. Lampen. 1968. Comparitive study of the properties of the purified internal and external invertases from yeast. *J. Biol. Chem.* 243:1573–1577.

Geli, M.I., and H. Riezman. 1996. Role of type I myosins in receptor-mediated endocytosis in yeast. *Science (Wash. DC).* 272:533–535.

Goodson, H.V., and J.A. Spudich. 1995. Identification and molecular characterization of a yeast myosin I. *Cell Motil. Cytoskeleton.* 30:73–84.

Gottlieb, T.A., I.E. Ivanov, M. Adesnik, and D.D Sabatini. 1993. Actin microfilaments play a critical role in endocytosis at the apical but not the basolateral surface of polarized epithelial cells. *J. Cell Biol.* 120:695–710.

Govindan, B., R. Bowser, and P. Novick. 1995. The role of Myo2, a yeast class V myosin, in vesicular transport. *J. Cell Biol.* 128:1055–1068.

Helenius, A., I. Mellman, D. Wall, and A. Hubbard. 1983. Endosomes. *Trends Biochem. Sci.* 8:245–250.

Hemmaplardh, D., and E.H. Morgan. 1976. Transferrin uptake and release by reticulocytes treated with proteolytic enzymes and neuraminidase. *Biochim. Biophys. Acta.* 426:385–398.

Herman, P.K., and S.D. Emr. 1990. Characterization of VPS34, a gene required for vacuolar protein sorting and vacuole segregation in *Saccharomyces cerevisiae. Mol. Cell Biol.* 10:6742–6754.

Herzog, V., and M.G. Farquhar. 1983. Use of electron-opaque tracers for studies on endocytosis and membrane recycling. *Methods Enzymol.* 98:203–225.

Hewlett, L.J., A.R. Prescott and C. Watts. 1994. The coated pit and macropinocytic pathways serve distinct endosome populations. *J. Cell Biol.* 124:689–703.

Ho, M.N., K.J. Hill, M.A. Lindorfer, and T.H. Stevens. 1993. Isolation of vacuolar membrane H(+)-ATPase-deficient yeast mutants: the VMA5 and VMA4 genes are essential for assembly and activity of the vacuolar H(+)-ATPase. *J. Biol. Chem.* 268:221–227.

Holtzman, D.A., S. Yang, and D.G. Drubin. 1993. Synthetic-lethal interactions identify two novel genes, SLA1 and SLA2, that control membrane cytoskeleton assembly in *Saccharomyces cerevisiae. J. Cell Biol.* 122:635–644.

Jansen, R.P., C. Dowzer, C. Michaelis, M. Galova, and K. Nasmyth. 1996. Mother cell-specific HO expression in budding yeast depends on the unconventional myosin myo4p and other cytoplasmic proteins [see comments]. *Cell.* 84:687–697.

Johnston, G.C., J.A. Prendergast, and R.A. Singer. 1991. The Saccharomyces cerevisiae MYO2 gene encodes an essential myosin for vectorial transport of vesicles. *J. Cell Biol.* 113:539–551.

Karin, M., and B. Mintz. 1981. Receptor-mediated endocytosis of transferrin in developmentally totipotent mouse teratocarcinoma stem cells. *J. Biol Chem.* 256:3245–3252.

Kilmartin, J.V., and A.E. Adams. 1984. Structural rearrangements of tubulin and actin during the cell cycle of the yeast *Saccharomyces. J. Cell Biol.* 98: 922–933.

Kubler, E., and H. Riezman. 1993. Actin and fimbrin are required for the internalization step of endocytosis in yeast. *EMBO (Eur. Mol. Biol. Organ.) J.* 12: 2855–2862.

Kubler, E., F. Schimmoller, and H. Riezman. 1994. Calcium-independent calmodulin requirement for endocytosis in yeast. *EMBO (Eur. Mol. Biol. Organ.) J.* 13:5539–5546.

Lamaze, C., and S.L. Schmid. 1995. The emergence of clathrin-independent pinocytic pathways. *Curr. Opin. Cell Biol.* 7:573–580.

Lemmon, S.K., V.P. Lemmon, and E.W. Jones. 1988. Characterization of yeast clathrin and anticlathrin heavy-chain monoclonal antibodies. *J. Cell Biochem.* 36:329–340.

Liu, H. and A. Bretscher. 1992. Characterization of TPM1 disrupted yeast cells indicates an involvement of tropomyosin in directed vesicular transport. *J. Cell Biol.* 118:285–299.

Miller, J. 1972. Experiments in Molecular Genetics Pages. Cold Spring Harbor Laboratory Press, Cold Spring Harbor, NY. 431–435.

Mueller, S.C., and D. Branton. 1984. Identification of coated vesicles in *Saccharomyces cerevisiae. J. Cell Biol.* 98:341–346.

Mulholland, J., D. Preuss, A. Moon, A. Wong, D. Drubin, and D. Botstein. 1994. Ultrastructure of the yeast actin cytoskeleton and its association with the plasma membrane. *J. Cell Biol.* 125:381–391.

Munn, A.L., and H. Riezman. 1994. Endocytosis is required for the growth of vacuolar H(+)-ATPase-defective yeast: identification of six new END genes. *J. Cell Biol.* 127:373–386.

Munn, A.L., B.J. Stevenson, M.I. Geli, and H. Riezman. 1995. end5, end6, and end7: mutations that cause actin delocalization and block the internalization step of endocytosis in *Saccharomyces cerevisiae. Mol. Biol. Cell.* 6:1721–1742.

Murphy, R.F., E.D. Jorgensen, and C.R. Cantor. 1982. Kinetics of histone endocytosis in Chinese hamster ovary cells. *J. Biol. Chem.* 257:1695–1701.

Nasmyth, K. 1993. Regulating the HO endonuclease in yeast. *Curr. Opin. Genet. Dev.* 3:286–294.

Nelson, H. and N. Nelson. 1990. Disruption of genes encoding subunits of yeast vacuolar H(+)-ATPase causes conditional lethality. *Proc. Natl. Acad. Sci. USA.* 87:3503–3507.

Novick, P., and D. Botstein. 1985. Phenotypic analysis of temperature-sensitive yeast actin mutants. *Cell.* 40:405–416.

Ottosen, P.D., P.J. Courtoy, and M.G. Farquhar. 1980. Pathways followed by membrane recovered from the surface of plasma cells and myeloma cells. *J. Exp. Med.* 152:1–19.

Palade, G.E. 1953. The fine structure of blood capillaries. *J. Appl. Physiol.* 24: 1424.

Parton, R.G., B. Joggerst, and K. Simons. 1994. Regulated internalization of caveolae. *J. Cell Biol.* 127:1199–1215.

Payne, G.S., and R. Schekman, 1985. A test of clathrin function in protein secretion and cell growth. *Science (Wash. DC).* 230:1009–1014.

Payne, G.S., T.B. Hasson, M.S. Hasson, and R. Schekman. 1987. Genetic and biochemical characterization of clathrin-deficient *Saccharomyces cerevisiae. Mol. Cell Biol.* 7:3888–3898.

Payne, G.S., D. Baker, E. van Tuinen, and R. Schekman. 1988. Protein transport to the vacuole and receptor-mediated endocytosis by clathrin heavy chain-deficient yeast. *J. Cell Biol.* 106:1453–1461.

Pearse, B.M., and R.A. Crowther. 1987. Structure and assembly of coated vesicles. *Annu. Rev. Biophys. Biophys. Chem.* 16:49–68.

Raths, S., J. Rohrer, F. Crausaz, and H. Riezman. 1993. end3 and end4: two mutants defective in receptor-mediated and fluid-phase endocytosis in *Saccharomyces cerevisiae. J. Cell Biol.* 120:55–65.

Ren, R., B.J. Mayer, P. Cicchetti, and D. Baltimore. 1993. Identification of a ten-amino acid proline-rich SH3 binding site. *Science (Wash. DC).* 259:1157–1161.

Rieder, S.E., L.M. Banta, K. Kohrer, J.M. McCaffery, and S.D. Emr. 1996. Multilamellar endosome-like compartment accumulates in the yeast vps28 vacuolar protein sorting mutant. *Mol. Biol. Cell.* 7:985–999.

Robinson, J.S., D.J. Klionsky, L.M. Banta, and S.D. Emr. 1988. Protein sorting in *Saccharomyces cerevisiae*: isolation of mutants defective in the delivery and processing of multiple vacuolar hydrolases. *Mol. Cell Biol.* 8:4936–4948.

Rose, M.D., P. Novick, J.H. Thomas, D. Botstein, and G.R. Fink. 1987. A *Saccharomyces cerevisiae* genomic plasmid bank based on a centromere-containing shuttle vector. *Gene (Amst.).* 60:237–243.

Rose, M.D., F. Winston, and P. Hieter. 1990. Methods in Yeast Genetics: A Laboratory Course Manual. Cold Spring Harbor Laboratory Press, Cold Spring Harbor, NY. 11–18.

Rothberg, K.G., J.E. Heuser, W.C. Donzell, Y.S. Ying, J.R. Glenney, and R.G. Anderson. 1992. Caveolin, a protein component of caveolae membrane coats. *Cell.* 68:673–682.

Rothberg, K.G., Y.S. Ying, J.F. Kolhouse, B.A. Kamen, and R.G. Anderson. 1990. The glycophospholipid-linked folate receptor internalizes folate without entering the clathrin-coated pit endocytic pathway. *J. Cell Biol.* 110:637–649.

Russo, P., N. Kalkkinen, H. Sareneva, J. Paakkola, and M. Makarow. 1992. A heat shock gene from *Saccharomyces cerevisiae* encoding a secretory glycoprotein [published erratum appears in *Proc. Natl. Acad. Sci. USA.* 1992. 89: 8857]. *Proc. Natl. Acad. Sci. USA.* 89:3671–3675.

Sachs, A.B. and J.A. Deardorff. 1992. Translation initiation requires the PAB-dependent poly(A) ribonuclease in yeast. *Cell.* 70:961–973.

Sandvig, K. and B. van Deurs. 1994. Endocytosis without clathrin. *Trends Cell Biol.* 4:275–277.

Schumacher, C., B.S. Knudsen, T. Ohuchi, P.P. Di Fiore, R.H. Glassman, and H. Hanafusa. 1995. The SH3 domain of Crk binds specifically to a conserved proline-rich motif in Eps15 and Eps15R. *J. Biol Chem.* 270:15341–15347.

Seaman, M.N.J., C.G. Burd, and S.D. Emr. 1996. Receptor signalling and the regulation of endocytic membrane transport. *Curr. Opin. Cell Biol.* 8:549–556.

Sheetz, M.P., and J. Dai. 1996. Modulation of membrane dynamics and cell motility by membrane tension. *Trends Cell Biol.* 6:85–89.

Sherman, F., G.R. Fink, and L.W. Lawrence. 1979. Methods in Yeast Genetics: A Laboratory Manual. Cold Spring Harbor Laboratory Press, Cold Spring Harbor, NY. 1–98.

Shortle, D., P. Novick, and D. Botstein. 1984. Construction and genetic characterization of temperature-sensitive mutant alleles of the yeast actin gene. *Proc. Natl. Acad. Sci. USA.* 81:4889–4893.

Singer, B., and H. Riezman. 1990. Detection of an intermediate compartment involved in transport of alpha-factor from the plasma membrane to the vacuole in yeast. *J. Cell Biol.* 110:1911–1922.

Sivadon, P., F. Bauer, M. Aigle, and M. Crouzet. 1995. Actin cytoskeleton and budding pattern are altered in the yeast rvs161 mutant: the Rvs161 protein shares common domains with the brain protein amphiphysin. *Mol. Gen. Genet.* 246:485–495.

Smythe, E., L.L. Carter, and S.L. Schmid. 1992. Cytosol- and clathrin-dependent stimulation of endocytosis in vitro by purified adaptors. *J. Cell Biol.* 119:1163–1171.

Stevens, T., B. Esmon, and R. Schekman. 1982. Early stages in the yeast secretory pathway are required for transport of carboxypeptidase Y to the vacuole. *Cell.* 30:439–448.

Tan, P.K., N.G. Davis, G.F. Sprague, and G.S. Payne, 1993. Clathrin facilitates the internalization of seven transmembrane segment receptors for mating pheromones in yeast. *J. Cell Biol.* 123:1707–1216.

Tang, H.-Y., and M. Cai. 1996. The EH-domain-containing protein Pan1 is required for normal organization of the actin cytoskeleton in *Saccharomyces cerevisae. Mol. Cell Biol.* 16:4897–4914.

Vida, T.A., and S.D. Emr. 1995. A new vital stain for visualizing vacuolar membrane dynamics and endocytosis in yeast. *J. Cell Biol.* 128:779–792.

Voss, H., J. Tamames, C. Teodoru, A. Valencia, C. Sensen, S. Wiemann, C. Schwager, J. Zimmermann, C. Sander, and W. Ansorge. 1995. Nucleotide sequence and analysis of the centromeric region of yeast chromosome IX. *Yeast.* 11:61–78.

Wang, Y.-X., H. Zhao, T.M. Harding, D.S. Gomes de Mesquita, C.L. Woldringh, D.J. Klionsky, A.L. Munn, and L.S. Weisman. 1996. Multiple classes of yeast mutants are defective in vacuole partitioning yet target vacuole proteins correctly. *Mol. Biol. Cell.* 7:1375–1389.

West, M.A., M.S. Bretscher, and C. Watts. 1989. Distinct endocytotic pathways in epidermal growth factor–stimulated human carcinoma A431 cells [published erratum appears in *J. Cell Biol.* 1990. 110:859]. *J. Cell Biol.* 109:2731–2739.

Willingham, M.C. and I.H. Pastan. 1982. Transit of epidermal growth factor through coated pits of the Golgi system. *J. Cell Biol.* 94:207–212.

Wong, W.T., C. Schumacher, A.E. Salcini, A. Romano, P. Castagnino, P.G. Pelicci, and P. Di Fiore. 1995. A protein-binding domain, EH, identified in the receptor tyrosine kinase substrate Eps15 and conserved in evolution. *Proc. Natl. Acad. Sci. USA.* 92:9530–9534.

Yanisch-Perron, C., J. Vieira, and J. Messing. 1985. Improved M13 phage cloning vectors and host strains: nucleotide sequences of the M13mp18 and pUC19 vectors. *Gene (Amst.).* 33:103–119.

Yu, H., J.K. Chen, S. Feng, D.C. Dalgarno, A.W. Brauer, and S.L. Schreiber. 1994. Structural basis for the binding of proline-rich peptides to SH3 domains. *Cell.* 76:933–945.

Zoladek, T., G. Vaduva, L.A. Hunter, M. Boguta, B.D. Go, N.C. Martin, and A.K. Hopper. 1995. Mutations altering the mitochondrial-cytoplasmic distribution of Mod5p implicate the actin cytoskeleton and mRNA 3′ ends and/or protein synthesis in mitochondrial delivery. *Mol. Cell Biol.* 15:6884–6894.